



Ice Accretion Formations on a NACA 0012 Swept Wing Tip in Natural Icing Conditions

Mario Vargas, Julius A. Giriunas, and Thomas P. Ratvasky
Glenn Research Center, Cleveland, Ohio

The NASA STI Program Office . . . in Profile

Since its founding, NASA has been dedicated to the advancement of aeronautics and space science. The NASA Scientific and Technical Information (STI) Program Office plays a key part in helping NASA maintain this important role.

The NASA STI Program Office is operated by Langley Research Center, the Lead Center for NASA's scientific and technical information. The NASA STI Program Office provides access to the NASA STI Database, the largest collection of aeronautical and space science STI in the world. The Program Office is also NASA's institutional mechanism for disseminating the results of its research and development activities. These results are published by NASA in the NASA STI Report Series, which includes the following report types:

- **TECHNICAL PUBLICATION.** Reports of completed research or a major significant phase of research that present the results of NASA programs and include extensive data or theoretical analysis. Includes compilations of significant scientific and technical data and information deemed to be of continuing reference value. NASA's counterpart of peer-reviewed formal professional papers but has less stringent limitations on manuscript length and extent of graphic presentations.
- **TECHNICAL MEMORANDUM.** Scientific and technical findings that are preliminary or of specialized interest, e.g., quick release reports, working papers, and bibliographies that contain minimal annotation. Does not contain extensive analysis.
- **CONTRACTOR REPORT.** Scientific and technical findings by NASA-sponsored contractors and grantees.

- **CONFERENCE PUBLICATION.** Collected papers from scientific and technical conferences, symposia, seminars, or other meetings sponsored or cosponsored by NASA.
- **SPECIAL PUBLICATION.** Scientific, technical, or historical information from NASA programs, projects, and missions, often concerned with subjects having substantial public interest.
- **TECHNICAL TRANSLATION.** English-language translations of foreign scientific and technical material pertinent to NASA's mission.

Specialized services that complement the STI Program Office's diverse offerings include creating custom thesauri, building customized data bases, organizing and publishing research results . . . even providing videos.

For more information about the NASA STI Program Office, see the following:

- Access the NASA STI Program Home Page at <http://www.sti.nasa.gov>
- E-mail your question via the Internet to help@sti.nasa.gov
- Fax your question to the NASA Access Help Desk at 301-621-0134
- Telephone the NASA Access Help Desk at 301-621-0390
- Write to:
NASA Access Help Desk
NASA Center for Aerospace Information
7121 Standard Drive
Hanover, MD 21076



Ice Accretion Formations on a NACA 0012 Swept Wing Tip in Natural Icing Conditions

Mario Vargas, Julius A. Giriunas, and Thomas P. Ratvasky
Glenn Research Center, Cleveland, Ohio

Prepared for the
40th Aerospace Sciences Meeting and Exhibit
sponsored by the American Institute of Aeronautics and Astronautics
Reno, Nevada, January 14–17, 2002

National Aeronautics and
Space Administration

Glenn Research Center

Acknowledgments

The authors would like to thank all of the personnel at Aircraft Operations for their help in all phases of the experiment and Mr. Chris Lynch from the Imaging Technology Center for his assistance with the photographic work.

Available from

NASA Center for Aerospace Information
7121 Standard Drive
Hanover, MD 21076

National Technical Information Service
5285 Port Royal Road
Springfield, VA 22100

Available electronically at <http://gltrs.grc.nasa.gov/GLTRS>

ICE ACCRETION FORMATIONS ON A NACA 0012 SWEEP WING TIP IN NATURAL ICING CONDITIONS

Mario Vargas[†], Julius A. Giriunas^{**}, Thomas P. Ratvasky^{***}

NASA Glenn Research Center, Cleveland, Ohio

Abstract

An experiment was conducted in the DeHavilland DHC-6 Twin Otter Icing Research Aircraft at NASA Glenn Research Center to study the formation of ice accretions on swept wings in natural icing conditions. The experiment was designed to obtain ice accretion data to help determine if the mechanisms of ice accretion formation observed in the Icing Research Tunnel are present in natural icing conditions. The experiment in the Twin Otter was conducted using a NACA 0012 swept wing tip. The model enabled data acquisition at 0°, 15°, 25°, 30°, and 45° sweep angles. Casting data, ice shape tracings, and close-up photographic data were obtained. The results showed that the mechanisms of ice accretion formation observed in-flight agree well with the ones observed in the Icing Research Tunnel. Observations on the end cap of the airfoil showed the same strong effect of the local sweep angle on the formation of scallops as observed in the tunnel.

Nomenclature

Λ	Sweep angle, degrees
d_{cr}	Critical distance, millimeters
<i>FSSP</i>	Forward Scattering Spectrometry Probe
<i>LWC</i>	Cloud liquid water content, g/m ³
<i>MVD</i>	Water droplet median volume diameter, μm
T	Temperature, °F
τ	Ice accretion time, minutes
V	Velocity, mph

* Aerospace Engineer, Icing Branch, NASA Glenn Research Center, Member AIAA

** Aerospace Engineer, Icing Branch, NASA Glenn Research Center, Member AIAA

*** Aerospace Engineer, Icing Branch, NASA Glenn Research Center, Member AIAA

Copyright © 2002 by the American Institute of Aeronautics and Astronautics, Inc. No copyright is asserted in the United States under Title 17, U.S. Code. The U.S. Government has a royalty-free license to exercise all rights under the copyright claimed herein for Governmental Purposes. All other rights are reserved by the copyright owner

Introduction

Past experimental investigations on the formation of ice accretions on swept wings at glaze ice conditions provided understanding of the mechanisms of formation, the role of local effects on roughness elements, the role of feather growth, and allowed identification of some of the important parameters involved. Since nearly all of those investigations were conducted in icing tunnels, it is critical to determine if the formation of ice accretions in natural icing conditions (in-flight) shows the same mechanisms observed in tunnel experiments.

This report presents the results of an experimental investigation carried out in the DeHavilland DHC-6 Twin Otter Icing Research Aircraft at NASA Glenn Research Center to study the formation of ice accretions on swept wings in natural icing conditions. The experiment in the Twin Otter was conducted using a swept NACA 0012 wing tip. The model enabled data acquisition at 0°, 15°, 30°, and 45° sweep angles. When the plane was in icing conditions, a hatch port on the upper part of the fuselage of the plane was opened and the airfoil was moved into the air stream using a specially designed stand. After the ice encounter the airfoil was lowered back into the aircraft cabin, and photographic data was taken at a location on the leading edge and along the end cap of the airfoil. After the photographic data was taken, ice tracings were made and the ice accretion was removed and stored in a freezer. At the end of the flight, a wax mold was made of each ice accretion. Later a casting of the ice accretion was obtained from the wax mold. Over a period of two and half weeks, data was obtained from 25 icing encounters.

Previous work on ice accretions in a natural icing environment on a swept wing was done by Reehorst¹. He conducted an experiment in the DeHavilland DHC-6 Twin Otter Icing Research Aircraft using a swept NACA 0012 wing tip airfoil. He obtained ice tracings and photographic data. The sweep angles employed were 0°, 30° and 45°.

He reported that the ice accretions were mostly of the glaze type and he observed scallop formations at 30° and 45° sweep angles. LEWICE 3D was modified and code predictions were compared to ice accretion flight data.

The presence of scallop formations on swept wings has been documented in past studies of ice accretions on swept wings^{2,3,4}. Reehorst and Bidwell⁵ did an experiment in the NASA Glenn Icing Research Tunnel (IRT) to study the effect of tunnel parameters on the presence or absence of scallops. Hedde and Guffond⁶ proposed a ballistic model of scallop growth.

A study of the fundamental physical mechanisms that lead to the formation of scallops on swept wings was conducted by Vargas and Reshotko^{7, 8}. They also conducted a parametric experimental study on the effect of velocity and sweep angle on the critical distance d_{cr} ⁹ and a study on the effect of LWC and temperature¹⁰ on the critical distance.

The present work continues the investigations into the formation of ice accretions on swept wings by studying the formation of these ice accretions in-flight.

Background

Previous studies on formation of ice accretions on swept wings at glaze ice conditions^{7,8} found that scallop and incomplete scallop formation is governed by local effects on roughness elements. Roughness elements formed at the beginning of the ice accretion process develop into glaze ice feathers when they reach a given height, and are located beyond a given distance from the attachment line. This distance is called the critical distance d_{cr} (see figure 1), and it depends on sweep angle and tunnel conditions¹⁰. When the critical distance is not zero it defines two zones on the ice accretion. A zone called the attachment line zone, where the roughness elements do not become feathers, and another zone called the glaze ice feathers zone where the roughness elements develop into feathers (figures 1a, 1b). The attachment line zone begins at the attachment line proper (the line in the spanwise direction, along which the flow splits over and under a wing) and extends on each side to the location where roughness elements develop into feathers (beginning of the glaze ice feathers zone). The glaze ice feathers zone begins at the end of the attachment line zone and extends some distance chordwise. Only feathers that are an active part of the main ice accretion are included in the

definition of the glaze ice feathers zone. When the critical distance is zero only the glaze ice feathers zone is present.

The feathers in the glaze ice feathers zone are inclined into the flow¹⁰. They have a tooth shape, and therefore a preferred direction of growth (the direction along which a feather is growing faster laterally, that is, the direction of the larger axis for the tooth shape of the top of the feather). The preferred direction of growth is oriented perpendicular to the external streamlines. The angle that the preferred direction of growth makes with respect to the attachment line direction is 90° for feathers located on the attachment line (streamlines are parallel to the attachment line direction at this location). The angle decreases as the distance from the attachment line increases (the streamlines are turning as they move away from the location of the attachment line).

Three types of ice accretions were identified on swept wings at glaze ice conditions: complete scallops, incomplete scallops, and no-scallops.

When complete scallops form¹⁰ (figure 2a), the ice accretion is covered with glaze ice feathers with a preferred direction of growth that is perpendicular to the external streamlines. The feathers have developed from roughness elements that reached a certain height. The value of the critical distance is zero, and only the glaze ice feathers zone is present. The feathers join along the preferred direction of growth to form ridges, with incipient scallop tips formed by the feathers at the end of each ridge. As the ridges grow they form scallop tips. The scallop tips have different inclinations with respect to the surface of the airfoil. Because of their different inclinations, as the scallop tips grow in height and along the preferred direction, they merge with adjacent scallop tips by joining at the top of the feathers that form each scallop tip. This mechanism is responsible for the growth of the scallop tips, their increase in size, and the enhancing of the spacing between scallops. Along the attachment line area the feathers tend to join other feathers around them by touching, bridging and filling, in this way they form areas of solid ice that are also covered with roughness elements. As the scallop tips grow by joining at their tops, the top surface tends to fill with water and areas of solid ice can be observed with roughness elements present.

When the critical distance is not zero and only roughness elements located beyond a given distance from the attachment line grow to become feathers,

incomplete scallops or no-scallops may develop. The formation of incomplete scallops or no-scallops depends on the angle that the preferred direction of growth of the feathers makes with respect to the attachment line direction.

When incomplete scallops form¹⁰ (figure 2b), the feathers in the glaze ice feathers zone will form scallop tips. The mechanisms of formation of these scallop tips were found to be identical to the mechanisms observed for the formation of the scallop tips in the complete scallop case. The formation of the scallop tips depends on the angle that the preferred direction of growth of the feathers makes with respect to the attachment line, which in turn depends on the distance from the attachment line at which those feathers are located. The angle must be large enough to allow the mechanisms of formation of scallop tips to operate and form scallop tips, and also must be large enough to prevent the ice of the attachment line zone from covering all the glaze ice feathers zone and burying the incipient scallop tips.

When no-scallops form¹⁰ (figure 2c), scallop tips are not present in the ice accretion. Three situations may lead to the formation of no-scallops. In one case the critical distance may be so large that only the attachment line zone is present. In the second case the attachment line zone and the glaze ice feathers zone are both present, but the angle of the feathers with respect to the attachment line direction is not large enough for the mechanisms of formation of scallop tips to operate. In the last case, the attachment line zone and the glaze ice feathers zone are both present, and the angle of the feathers with respect to the attachment line direction is large enough for the mechanisms of scallop tip formation to operate, but not large enough to prevent the ice of the attachment line from totally covering the scallop tips. When the feathers are totally covered they cease to play a role in the formation of the ice accretion.

When the attachment line zone and the glaze ice feathers zone are both present, in general one will tend to prevail over the other in the first stages of the formation of the ice accretion, and this will influence the final ice shape. This interaction between the ice of the attachment line zone and the feathers in the glaze ice feathers zone depends on how fast each kind of ice grows. In an incomplete scallop when the critical distance is small and the feathers in the glaze ice feathers zone grow faster than the ice of the attachment line, they will form large scallop tips. As ice accretion time increases the large scallop tips wash out the presence of the attachment line zone

and the ice accretion looks almost like complete scallops. In a no-scallop, in some cases the feathers may grow faster than the attachment line ice in the beginning of the ice accretion, but the ice of the attachment line eventually will cover them and the feathers will cease to play a role in the formation of the ice shape. Because of the fast growth of the feathers in the initial stage of the formation of the ice accretion, the ice shape will show horns, and resemble some of the ice shapes that are observed in 2D ice accretions.

In all cases of formation of glaze ice accretions on a swept wing, the distance from the attachment line beyond which the roughness elements become glaze ice feathers (the critical distance d_{cr}) is a critical factor in the kind of ice accretion that will form.

A Parametric experimental study on the effect of velocity and sweep angle on the critical distance⁹ conducted on a swept NACA 0012 wing tip showed that at a given velocity and tunnel condition, as the sweep angle is increased from 0° to 25°, the critical distance slowly decreases. As the sweep angle is increased past 25°, the critical distance starts decreasing more rapidly. For 75 and 100 mph it reaches a value of 0 millimeters at 35°. For 150 and 200 mph it reaches a value of 0 millimeters at 40°. On the ice accretion, as the sweep angle is increased from 0° to 25°, the extent of the attachment line zone slowly decreases but overall, the ice accretions remain similar to the 0° sweep angle case. As the sweep angle is increased above 25°, the extent of the attachment line zone decreases rapidly and complete scallops form at 35° sweep angle for 75 and 100 mph, and at 40° for 150 and 200 mph.

A study on the effect of LWC and temperature on the critical distance¹⁰ conducted on a swept NACA 0012 wing tip airfoil found that decreasing the LWC to 0.5 g/m³ decreases the value of the critical distance at a given sweep angle compared to the baseline case, and starts the formation of complete scallops at 30° sweep angle. Increasing the LWC to 1.0 g/m³ increases the value of the critical distance compared to the baseline case, the critical distance remains always above 0 millimeters and complete scallops are not formed. Decreasing the total temperature to 20 °F decreases the critical distance with respect to the baseline case and formation of complete scallops begins at 25° sweep angle. When the total temperature was increased to 30 °F, bumps covered with roughness elements appear on the ice accretion at 25° and 30° sweep angles, large ice structures appear at 35° and 40°

sweep angles, and complete scallops are formed at 45° sweep angle.

Experimental Procedure

Icing Research Aircraft

The icing research aircraft is a modified DeHavilland DHC-6 Twin Otter Icing Research Aircraft (figure 3). It is a twin engine commuter type aircraft powered by two 550 shaft horsepower turboprop engines. It has been modified for flight in icing environments and to permit the acquisition of icing data.

Instrumentation and Data Reduction

The Twin Otter Icing Research Aircraft is equipped with standard flight instrumentation and with instrumentation specific to icing research. The measured flight data consisted of airspeed, outside air temperature, angle of attack, angle of sideslip, droplet size (MVD), liquid water content (LWC), and altitude. The LWC was measured using a King probe. Droplet size (MVD) measured by a Forward Scattering Spectrometry Probe (FSSP). The outside temperature was measured with a Rosemount probe mounted on the fuselage. Airspeed, altitude, angle of attack and sideslip were measured with a Rosemount 858 probe.

All data was acquired using Science Engineering and Associates (SEA) M200 data acquisition software and was stored in a binary format. SEA Playback software read the binary formatted data and produced ASCII files which were analyzed using a spreadsheet software. The time series for each parameter was plotted and time averages and standard deviations were calculated. Table 1 shows the summary of the flight data.

Model and Related Hardware

The model chosen for this study was a NACA 0012 swept wing tip (figure 4). The airfoil is made of wood, with a 0.381-meter (15-inch) chord measured normal to the leading edge, and a 0.609-meter (24-inch) span. It was fitted with a rounded end cap. It was mounted on a base that allowed pivoting of the airfoil to sweep angles from 0° to 45° in 5° increments. The base of the airfoil was attached to a specially designed stand (figure 5). The stand consisted of a system of pulleys connected to a crank that allowed the airfoil to be raised through a

hatch in the cabin of the aircraft and into the airstream.

A heater was installed on the area where the measurements and collection of ice shapes were going to be performed. The heater was powered by a 28 DC, 1 amp, power supply. A grid was painted on the surface of the heater to allow identification of the flow direction on the photographic data and to serve as a distance scale in some pictures.

A small laboratory type freezer (figure 5) was used to store the ice samples during flight operations. The freezer weighs 60 lbs and has 1.5 cu-ft of storage. It draws a peak current of 11 amps at startup, but rapidly drops to 1 amp during continuous operation. The freezer uses a small amount of R-134A refrigerant as the working fluid and can maintain the ice samples between -4° and 20° F. Ice samples were laid on bubble-wrap material to prevent damage to them during storage. The freezer door was modified with a safety latch to keep it securely closed while in flight and during take-offs/landings. Ice packs were also installed in the freezer to help keep ice samples frozen in the event the power to the freezer was interrupted for any extended period of time.

Test Procedure

Each day of testing started with identification of icing conditions. The pilots and the test engineer held a telecon with National Center for Atmospheric Research personnel to determine the best altitude and location to intercept icing conditions. The aircraft was launched. When the location for icing conditions was reached a determination was made if the conditions were sufficient or if better icing conditions were needed. If better icing conditions were needed, communication was established by Satcom with NCAR personnel, and a better location for icing conditions was located (if it existed). If the conditions were found to be sufficient, a holding pattern was established and the experiment was started. The hatch on the ceiling of the aircraft was opened, and the airfoil was elevated through the hatch into the airstream.

Because of the size of the hatch opening, the airfoil was elevated at 0° sweep angle through the hatch and once in the airstream it was set at the selected sweep angle. The starting time for the icing encounter was recorded. During the icing

conditions the meteorological data was recorded by the data acquisition system and constantly monitored by the test engineer. About midpoint into the ice encounter, the researcher requested from the test engineer a reading of the meteorological conditions and wrote them in a data sheet, these conditions were used as a rough indication of the icing conditions.

Once the ice accretion was formed, the airfoil was moved to 0° sweep angle and lowered into the cabin. The ending time of the ice encounter was recorded. Photographic data of the ice accretion was taken. Three cuts were made in the ice accretion using an aluminum template. The cuts were made perpendicular to the leading edge. A cardboard tracing was made in the middle cut. Once the tracing was done, the heater was activated and two samples of the ice accretion were removed from the airfoil and placed in a freezer. The freezer was kept at a temperature near 10 °F. The airfoil was cleaned and prepared for the next data point. At the end of the flight, the ice accretions were placed in a Styrofoam container and moved to the location in the hangar where a wax bath was maintained. A wax mold of each ice accretion was made and labeled. Later a casting of the ice accretion was obtained from the wax mold.

Castings

For each of the wax molds a urethane casting was made of the ice shape. The castings allowed measurement of the critical distance and observation of the ice accretion.

The castings were made by dipping the ice shape several times in a bath of bees-wax at 150 °F to form a wax mold, draining the water from inside the wax mold, and filling the mold with liquid urethane. The urethane was allowed to solidify, and then a solvent was used to remove the wax.

Results and Discussion

For the purpose of data analysis, the flight data was divided into four groups labeled A through D. The data in a given group have average icing conditions within a close range of values. This division of the data allowed observation of the effect of the sweep angle and in some cases comparison to Icing Research Tunnel data.

Table 1 presents the complete summary of the flight data. Tables 2 through 5 present the flight data in each one of the groups A through D.

Group A: glaze ice conditions

The data in this group (Table 2) have average icing conditions close to $V = 150$ mph, $T_{total} = 25$ °F, $LWC = 0.4$ g/m³, $MVD = 13$ μm.

For the in-flight test the sweep angles tested were 0°, 15°, 25°, 30°, and 45°.

For a sweep angle of 45° two ice accretions belong to group A (figures 6,7). The average conditions for both cases are about the same with slight difference in the LWCs (0.48 g/m³ versus 0.37 g/m³).

For the higher LWC (figure 6) the scallop tips are well defined and starting at the attachment line. The ice shape is a complete scallop. The scallop tips are very close and the spaces between are filled with ice. This ice shape is different from the ice shape in figure 7. The ice shape is almost identical to ice shapes obtained at a lower total temperature (figure 23) and also to an ice shape obtained at lower LWC (figure 20).

The ice shape in figure 7 is a complete scallop. A side view of the ice accretion (figure 8) shows the feather formation of the scallop tips. It compares well with an ice accretion obtained in the IRT (figure 9) at $\Lambda = 45^\circ$, $V = 150$ mph, $T_{total} = 25$ °F, $LWC = 0.5$ g/m³, $MVD = 20$ μm, $\tau = 5$ minutes. Close up photographic data of the in-flight accretion (figure 10) and the IRT accretion (figure 11) show that they share the same icing characteristics. The scallop tips are similar in formation and not well defined. They are made of feathers joining along their preferred direction of growth. In both ice accretions large feathers with a preferred direction growth can be seen along the attachment line. These large ice feathers along the attachment line have been observed in past studies of ice accretions on swept wings¹⁰. They typically start appearing at large sweep angles when the LWC is lowered from 0.75 g/m³ to 0.5 g/m³, or when the total temperature is lowered from 25 °F to 20 °F starting at a baseline condition of 150 mph, 25 °F, 0.75 g/m³, 20 μm MVD.

At a sweep angle of 30° the ice shape (figure 12) is a complete scallop. Comparison with an accretion obtained in the tunnel (figure 13) at $\Lambda = 30^\circ$, $V = 150$ mph, $T_{\text{total}} = 25^\circ\text{F}$, $\text{LWC} = 0.5 \text{ g/m}^3$, $\text{MVD} = 20 \mu\text{m}$, $\tau = 10$ minutes, shows that the two ice accretions have the same overall characteristics. For both ice accretions large feathers appear along the attachment line area. Only the top of the feathers can be observed and the space between them is filled by ice with roughness elements. The scallop tips are present in both cases but they are small and not well defined.

At a sweep angle of 15° the ice shape is a no-scallop (figure 14). Comparison with an ice accretion (figure 15) obtained in the tunnel at $\Lambda = 15^\circ$, $V = 150$ mph, $T_{\text{total}} = 25^\circ\text{F}$, $\text{LWC} = 0.5 \text{ g/m}^3$, and $\text{MVD} = 20 \mu\text{m}$, $\tau = 10$ minutes, shows that the two ice accretions share similar characteristics. In both cases the attachment line and the glaze ice feathers zone are present. In both cases the attachment line zones are covered with roughness elements. The feathers in the glaze ice feathers zones have a preferred direction of growth oriented in the direction of the attachment line. In both cases the critical distance (d_{cr}) is present. For the tunnel ice accretion $d_{\text{cr}} = 7$ mm, for the in-flight ice accretion $d_{\text{cr}} = 8$ mm.

At a sweep angle of 0° the ice accretion is a no scallop (figure 16). Comparison with an ice accretion (figure 17) obtained in the tunnel at $\Lambda = 0^\circ$, $V = 150$ mph, $T_{\text{total}} = 25^\circ\text{F}$, $\text{LWC} = 0.5 \text{ g/m}^3$, and $\text{MVD} = 20 \mu\text{m}$, $\tau = 5$ minutes, shows that the same icing characteristics are present. Both ice shapes have an attachment line zone covered with roughness elements and a reduced glaze ice feathers zone. For the in-flight ice shape $d_{\text{cr}} = 9$ mm, and for the tunnel ice shape $d_{\text{cr}} = 11.5$ mm.

Observations on the end cap of the airfoil allow studying the effect of changing the local sweep angle for the same icing conditions. This is especially important in the in-flight data because the conditions are unsteady. Figures 18 and 19 present the photographic data on the end cap when the airfoil was set a sweep angle of 15° . On the span of the airfoil the ice accretion is a no-scallop (figure 14). As the local sweep angle changes along the end cap of the airfoil, the critical distance collapses and scallops made of feathers with a preferred direction of growth can be observed (figure 18). A side view of the scallops on the end cap (figure 19) shows their feather formation. These observations are consistent with observations made in IRT experiments of how the

increase in the local sweep angles on the end cap affect the ice shape.

At the bottom of Table 2 there are three data points below the heading "Data points with lower LWCs". These data points have similar icing conditions to the other ones but the LWCs are closer to 0.3 g/m^3 than to 0.4 g/m^3 . The three points are for sweep angles of 45° , 30° , and 25° .

In the case for a sweep angle of 45° (figure 20) the ice accretion is similar to the ice accretion in figure 6. It is a complete scallop. Scallop tips are well defined. Ice is filling the space between the scallop tips.

In the case for a sweep angle of 30° (figure 21) the ice accretion is a complete scallop. The overall ice accretion is similar to the case with the higher LWC discussed above (figure 12), but the ice forming the ice shape is less transparent, more towards rime ice.

In the case for a sweep angle of 25° (figure 22), the ice accretion is an incomplete scallop. The scallop tips are present although not well defined. The attachment line zone and the glaze ice feathers zone can be observed. The attachment line zone is covered with large roughness elements. The tops of large ice feathers seen at larger sweep angles are not present.

Group B

The data in this group (Table 3) have average icing conditions close to $V = 150$ mph, $T_{\text{total}} = 20^\circ\text{F}$, $\text{LWC} = 0.5 \text{ g/m}^3$, $\text{MVD} = 12 \mu\text{m}$. The main difference with the data from group A is the lower total temperature of 20°F versus 25°F . The effect of lower temperature can be observed when comparing the ice accretions in both groups.

Icing test points were obtained for sweep angles of 45° , 30° , 15° and 0° .

For 45° sweep angle (figure 23) the ice accretion is a complete scallop. The ice accretion is similar to the ice shape in figure 6. Well-defined scallop tips can be observed. The space between the scallop tips and the area around the attachment line are covered with ice.

For 30° sweep angle (figure 24) the ice accretion looks similar to the ice accretion from group A for the same sweep angle but in this case the area around the attachment line is covered with ice (figure 25) and there is no indication of large

feathers. The attachment line zone and the glaze ice feathers zones are present. Side views of the ice accretion show that the feathers in the glaze ice feathers zone are tightly packed (figure 26). The ice shape is an incomplete scallop. The critical distance measured from the photographic data is 3 mm.

For 15° and 0° sweep angle (figures 27, 28) the ice shapes show the attachment line zone and the glaze ice feathers zone. In both cases the attachment line zone is covered with large roughness elements. The diameter of the roughness elements is of the order of 2 mm or less. In both cases the feathers in the glaze ice feathers zones are tightly packed, with the preferred direction of growth of the feathers aligned nearly parallel to the direction of the attachment line flow. Figure 29 shows the feathers for the 15° case. The critical distances measured from the photographic data are 6 mm and 10 mm for 15° and 0° sweep angles respectively.

Group C

The data in this group (Table 4) have average total temperatures close to 30 °F.

Two cases are for a sweep angle of 45°. One case has an average LWC of 0.36 g/m³ (figure 30). The ice accretion is a complete scallop made of glaze ice feathers. The other case for a sweep angle of 45° is for an LWC of 0.13 g/m³ (figure 31). At the lower LWC the ice accretion is more toward rime ice. This is especially evident in the color of the ice that is whitish and less transparent. The ice accretion is still a complete scallop.

One additional case was for a sweep angle of 0°. The ice accretion is a no scallop (figure 32), with roughness elements covering the attachment line zone.

In all cases observed, the effect of high temperature is not as marked as observed in tunnel experiments, but in the tunnel the cases were all at higher LWC. The effect of lowering the LWC is in some ways similar to lowering temperature.

Group D

The data in this group (Table 5) have average values of LWC less than 0.2 g/m³ and total temperatures close to 20 °F. Data were obtained for sweep angles of 45°, 30°, 15° and 0°.

The ice accretions for 0°, 15°, and 30° (figures 33, 34, 35) show similar icing characteristics. The attachment line zone and the glaze ice feathers zones are present in each case. The attachment line zones are clear and smooth. The icing conditions (low LWC and low temperature) are favorable to mixed ice and this is reflected in the ice in the attachment line zone. In all cases the feathers in the glaze ice feathers zone are tightly packed (figure 36) and tend to form a solid piece in the areas that are close to the end of the attachment line zone.

For 0° and 15° sweep angles the ice accretions are no scallops. For 30° some degree of scallop tips can be observed, the ice accretion is an incomplete scallop.

The critical distance for each sweep angle case is smaller than for the cases with similar average icing conditions but larger LWC discussed above (group B). This is consistent with observations from experiments in the IRT that indicated that the critical distance decreases as the LWC is decreased (other icing conditions maintained the same). The critical distances measured from the photographic data were: 3.5 mm, 3 mm, and 2 mm at sweep angles of 0°, 15° and 30° respectively.

For a sweep angle of 45° the ice accretion shows scallop tips (figure 37) with tightly packed feathers forming them (figure 38). In the area around the attachment line zone the ice looks like a solid piece. The ice accretion seems to be made of tightly packed feathers that fuse together or get covered by ice.

Conclusions

An experiment was conducted in the DeHavilland DHC-6 Twin Otter Icing Research Aircraft at NASA Glenn Research Center to study the formation of ice accretions on swept wings in natural icing conditions. The experiment was designed to obtain ice accretion data to help determine if the mechanisms of ice accretion formation observed in the Icing Research Tunnel are present in natural icing conditions.

The experimental investigation showed that in the case where the in-flight average icing condition was close to a tested tunnel icing condition and a comparison could be made, the ice accretions showed similar icing characteristics at each sweep angle tested. At 45° and 30° sweep angles the ice

accretions were complete scallops made of feathers with a preferred direction of growth. In particular, the presence of large feathers or the top of large feathers along the attachment line area agrees well with past tunnel observations at similar low LWC icing conditions. At 15° and 0° sweep angles the attachment line zone and the glaze ice feathers zone were present and the critical distance could be measured.

For the in-flight ice accretions the change in the ice shape as the local sweep angle increases along the end cap of the airfoil agrees well with tunnel observations.

In cases where no tunnel data were available to make a comparison, the in-flight ice accretions showed the same general elements of formation that have been observed in ice accretions obtained in tunnel experiments:

(i) The presence of the attachment line zone and/or a glaze ice feathers zone. This allows the ice accretions to be classified as no-scallops, incomplete scallops or complete scallops.

(ii) The presence of scallop tips made of feathers with a preferred direction of growth for complete and incomplete scallops

(iii) The presence of the attachment line zone and the glaze ice feathers zone for incomplete scallops and no-scallops.

(iv) The attachment line zone made of ice covered with roughness elements with diameters of the order of 2 millimeters or less when the conditions are favorable for glaze ice, or a clear smooth ice when the conditions are favorable to mixed ice.

(v) The presence of the critical distance and its decrease to zero as the sweep angle increases towards 45°.

The test results indicate that the formation of ice accretions on a swept NACA 0012 airfoil in-flight is consistent with what we know about the formation of ice accretions in the Icing Research Tunnel

Acknowledgements

The authors would like to thank all of the personnel at Aircraft Operations for their help in all phases of the experiment, and Mr. Chris Lynch from the Imaging Technology Center for his assistance with the photographic work.

References

¹ Reehorst, A.L., "Prediction of Ice Accretion on a Swept NACA 0012 Airfoil and Comparisons to Flight Test Results", *AIAA Paper 92-0043*, Jan. 1992.

² Pierre, M. and Vaucheret, X., "Icing Test Facilities and Test Techniques in Europe", *AGARD Report No. 127 (Aircraft Icing)*, Ottawa, Canada, 1977.

³ Laschka, B. and Jesse, R.E., "Ice Accretion and its Effects on Aerodynamics of Unprotected Aircraft Components", *AGARD Report No. 127 (Aircraft Icing)*, Ottawa, Canada, 1977.

⁴ Wilder, R.W., "A Theoretical and Experimental Means to Predict Ice Accretion Shapes for Evaluating Aircraft Handling and Performance Characteristics", *AGARD Report No. 127 (Aircraft Icing)*, Ottawa, Canada, 1977.

⁵ Reehorst, A.L. and Bidwell, C., NASA Lewis Research Center internal document, 1991.

⁶ Hedde, T. and Guffond, D., "Improvement of the ONERA 3D Icing Code, Comparison with 3D Experimental Shapes", *AIAA Paper 93-0169*, Jan. 1993.

⁷ Vargas, M. and Reshotko, E., "Physical Mechanisms of Glaze Ice Scallop Formations on Swept Wings", *AIAA Paper 98-0491*, Jan. 1998. *NASA TM-1998-206616*.

⁸ Vargas, M., "Ice Accretion on Swept Wings at Glaze Ice Conditions", *Ph.D. Thesis, Case Western Reserve University, Cleveland, Ohio, May 1998*.

⁹ Vargas, M. and Reshotko, E., "Parametric Experimental Study of the Formation of Glaze Ice Shapes on Swept Wings", *AIAA Paper 99-0094*, Jan. 1999. *NASA TM-1999-208900*.

¹⁰ Vargas, M. and Reshotko, E., "LWC and Temperature Effects on Ice Accretion Formation on Swept Wings at Glaze Ice Conditions", *AIAA Paper 2000-0483*, Jan. 2000. *NASA TM-2000-209777*.

Flight Number	Run number	Sweep Angle	Ice Accretion Time minutes	Velocity mph/(knots)	Total Temperature °F(°C)	Static Temperature °F(°C)	Beta Degrees	FSSP-MVD μm	King's LWC g/m ³	FSSP LWC g/m ³	FSSP total concentration #/cm ³	Pressure altitude meters/ (feet)
2001-04	011801.01	0°	15	151/(131)	16.9/(+8.4)	11.1/(-11.6)	-0.2	11	0.1	0.05	67	3541/(11616)
2001-05	011901.01	0°	32	138/(120)	19.0/(-7.2)	14.0/(-10.0)	-0.1	18	0.08	0.03	12	3819/(12531)
2001-05	011901.02	45°	22	132/(115)	18.3/(-7.6)	13.6/(-10.2)	-0.2	17	0.07	0.06	21	3861/(12666)
2001-06	011901.03	45°	14	143/(124)	25.0/(-3.9)	21.2/(-6.0)	0.0	14	0.33	0.15	119	866/(2807)
2001-06	011901.04	30°	19	142/(123)	19.6/(-6.9)	15.6/(-9.1)	-0.1	15	0.20	0.14	78.3	1371/(4497)
2001-06	011901.05	15°	18	137/(119)	19.4/(-7)	14.9/(-9.5)	0.3	14	0	0.16	105	1386/(4547)
2001-07	012201.01	45°	25	159/(138)	18.9/(-7.3)	14.2/(-9.9)	-0.2	9	0.14	0.09	217.5	1073/(3521)
2001-07	012201.02	30°	19	158/(137)	23.5/(-4.7)	18.9/(-7.3)	-0.1	6	0.10	0.06	144	1113/(3651)
2001-09	012401.01	45°	10	142/(123)	24.8/(-4.0)	21.0/(-6.1)	0.9	12.3	0.48	0.22	221	860/(2822)
2001-09	012401.02	30°	13	144/(125)	22.1/(-5.5)	18.1/(-7.7)	0.5	12.8	0.54	0.24	218	970/(3182)
2001-09	012401.03	15°	10	143/(124)	20.5/(-6.4)	16.7/(-8.5)	0.0	12.6	0.51	0.24	179	1045/(3428)
2001-09	012401.04	0°	9	142/(123)	21.2/(-6.0)	17.4/(-8.1)	0.0	12.1	0.46	0.23	166	1014/(3325)
2001-10	012401.05	0°	16	146/(127)	20.0/(-6.65)	16.0/(-8.89)	-0.26	10.20	0.28	0.13	162	1142/(3748)
2001-10	012401.06	15°	15	142/(123)	22.2/(-5.43)	18.4/(-7.55)	-0.10	11.44	0.31	0.15	176	1115/(3659)
2001-10	012401.07	45°	13	144/(125)	19.3/(-7.04)	15.4/(-9.22)	-0.30	11.82	0.40	0.24	275	1216/(3990)
2001-10	012401.08	30°	13	140/(122)	20.8/(-6.23)	17.0/(-8.32)	-0.09	10.67	0.31	0.20	255	1228/(4029)
2001-11	012601.01	45°	9	159/(138)	30.6/(-0.8)	25.5/(-3.6)	0.2	14.4	0.36	0.18	115	1541/(5057)
2001-11	012601.02	30°	12	139/(121)	26.2/(-3.2)	22.3/(-5.4)	0.4	13.5	0.32	0.15	105	1538/(5047)
2001-11	012601.03	0°	12	138/(120)	30.2/(-1.0)	26.4/(-3.1)	0.8	12.0	0.31	0.12	135	1204/(3951)
2001-13	013001.01	45°	41	148/(129)	29.3/(-1.5)	24.1/(-4.4)	-0.1	14.9	0.13	0.06	25	2787/(9143)
2001-14	013101.01	45°	6	142/(123)	26.6/(-3.0)	22.8/(-5.1)	-0.1	12.2	0.37	0.16	171	1280/(4201)
2001-14	013101.02	30°	8	144/(125)	25.3/(-3.7)	21.2/(-6.0)	-0.8	13.3	0.45	0.23	171	1594/(5231)
2001-14	013101.03	15°	8	143/(124)	25.9/(-3.4)	21.9/(-5.6)	-0.5	12.3	0.39	0.26	219	1435/(4709)
2001-14	013101.04	0°	7	142/(123)	26.4/(-3.1)	21.7/(-5.7)	-0.7	13.1	0.41	0.30	249	1388/(4553)
2001-14	013101.05	25°	7	143/(124)	26.1/(-3.3)	22.1/(-5.5)	-0.6	12.2	0.32	0.21	206	1390/(4560)

Table 1. Summary of Flight Data

Flight Number	Run number	Sweep Angle	Ice Accretion Time minutes	Velocity mph/(knots)	Total Temperature °F(°C)	Static Temperature °F(°C)	Beta degrees	FSSP-MVD μm	King1 LWC g/m ³	FSSP LWC g/m ³	FSSP total concentration #/cm ³	Pressure altitude meters/ (feet)
2001-09	012401.01	45°	10	142 / (123)	24.8 / (-4.0)	21.0 / (-6.1)	0.9	12.3	0.48	0.22	221	860 / (2822)
2001-14	013101.01	45°	6	142 / (123)	26.6 / (-3.0)	22.8 / (-5.1)	-0.1	12.2	0.37	0.16	171	1280 / (4201)
2001-14	013101.02	30°	8	144 / (125)	25.3 / (-3.7)	21.2 / (-6.0)	-0.8	13.3	0.45	0.23	171	1594 / (5231)
2001-14	013101.03	15°	8	143 / (124)	25.9 / (-3.4)	21.9 / (-5.6)	-0.5	12.3	0.39	0.26	219	1435 / (4709)
2001-14	013101.04	0°	7	142 / (123)	26.4 / (-3.1)	21.7 / (-5.7)	-0.7	13.1	0.41	0.30	249	1388 / (4553)
Data points with lower LWC:												
2001-14	013101.05	25°	7	143 / (124)	26.1 / (-3.3)	22.1 / (-5.5)	-0.6	12.2	0.32	0.21	206	1390 / (4560)
2001-11	012601.02	30°	12	139 / (121)	26.2 / (-3.2)	22.3 / (-5.4)	0.4	13.5	0.32	0.15	105	1538 / (5047)
2001-06	011901.03	45°	14	143 / (124)	25.0 / (-3.9)	21.2 / (-6.0)	0.0	14	0.33	0.15	119	856 / (2807)

Table 2. Data Group A: data with average icing conditions close to V = 150 mph, T_{total} = 25 °F, LWC = 0.4 g/m³, MVD = 13 μm

Flight Number	Run number	Sweep Angle	Ice Accretion Time minutes	Velocity mph/(knots)	Total Temperature °F(°C)	Static Temperature °F(°C)	Beta degrees	FSSP-MVD μm	King1 LWC g/m ³	FSSP LWC g/m ³	FSSP total concentration #/cm ³	Pressure altitude meters/ (feet)
2001-10	012401.07	45°	13	144 / (125)	19.3 / (-7.04)	15.4 / (-9.22)	-0.30	11.82	0.40	0.24	275	1216 / (3990)
2001-09	012401.02	30°	13	144 / (125)	22.1 / (-5.5)	18.1 / (-7.7)	0.5	12.8	0.54	0.24	218	970 / (3182)
2001-09	012401.03	15°	10	143 / (124)	20.5 / (-6.4)	16.7 / (-8.5)	0.0	12.6	0.51	0.24	179	1045 / (3428)
2001-09	012401.04	0°	9	142 / (123)	21.2 / (-6.0)	17.4 / (-8.1)	0.0	12.1	0.46	0.23	166	1014 / (3325)
Cases with lower LWC:												
2001-10	012401.06	15°	15	142 / (123)	22.2 / (-5.43)	18.4 / (-7.55)	-0.10	11.44	0.31	0.15	176	1115 / (3659)
2001-10	012401.08	30°	13	140 / (122)	20.8 / (-6.23)	17.0 / (-8.32)	-0.09	10.67	0.31	0.20	255	1228 / (4029)

Table 3. Data Group B: data with average icing conditions close to V = 150 mph, T_{total} = 20 °F, LWC = 0.5 g/m³, MVD = 12 μm

Flight Number	Run number	Sweep Angle	Ice Accretion Time minutes	Velocity mph/(knots)	Total Temperature °F/(°C)	Static Temperature °F/(°C)	Beta degrees	FSSP-MVD μm	King1 LWC g/m ³	FSSP LWC g/m ³	FSSP total concentration #/cm ³	Pressure altitude meters/ (feet)
2001-11	012601.01	45°	9	159 / (138)	30.6 / (-0.8)	25.5 / (-3.6)	0.2	14.4	0.36	0.18	115	1541 / (5057)
2001-11	012601.03	0°	12	138 / (120)	30.2 / (-1.0)	26.4 / (-3.1)	0.8	12.0	0.31	0.12	135	1204 / (3951)
2001-13	013001.01	45°	41	148 / (129)	29.3 / (-1.5)	24.1 / (-4.4)	-0.1	14.9	0.13	0.06	25	2787 / (9143)

Table 4. Data Group C: data with total temperature close to 30 °F

Flight Number	Run number	Sweep Angle	Ice Accretion Time minutes	Velocity mph/(knots)	Total Temperature °F/(°C)	Static Temperature °F/(°C)	Beta degrees	FSSP-MVD μm	King1 LWC g/m ³	FSSP LWC g/m ³	FSSP total concentration #/cm ³	Pressure altitude meters/ (feet)
2001-05	011901.02	45°	22	132 / (115)	18.3 / (-7.6)	13.6 / (-10.2)	-0.2	17	0.07	0.06	21	3861 / (12666)
2001-07	012201.01	45°	25	159 / (138)	18.9 / (-7.3)	14.2 / (-9.9)	-0.2	9	0.14	0.09	217.5	1073 / (3521)
2001-06	011901.04	30°	19	142 / (123)	19.6 / (-6.9)	15.6 / (-9.1)	-0.1	15	0.20	0.14	78.3	1371 / (4497)
2001-07	012201.02	30°	19	158 / (137)	23.5 / (-4.7)	18.9 / (-7.3)	-0.1	6	0.10	0.06	144	1113 / (3651)
2001-06	011901.05	15°	18	137 / (119)	19.4 / (-7)	14.9 / (-9.5)	0.3	14	0	0.16	105	1386 / (4547)
2001-04	011801.01	0°	15	151 / (131)	16.9 / (-8.4)	11.1 / (-11.6)	-0.2	11	0.1	0.05	67	3541 / (11616)
2001-05	011901.01	0°	32	138 / (120)	19.0 / (-7.2)	14.0 / (-10.0)	-0.1	18	0.08	0.03	12	3819 / (12531)
2001-10	012401.05	0°	16	146 / (127)	20.0 / (-6.65)	16.0 / (-8.89)	-0.26	10.20	0.28	0.13	162	1142 / (3748)

Table 5. Data Group D: data with average values of LWC less than 0.2 g/m³ and total temperature close to 20 °F

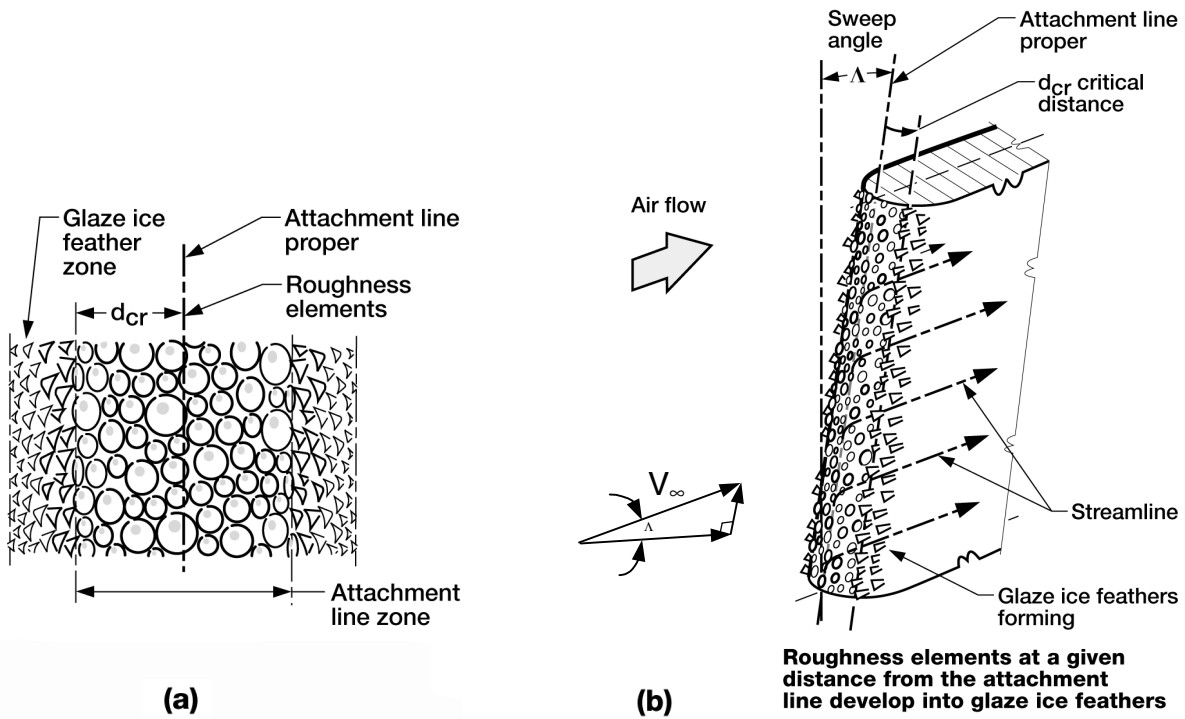


Figure 1. Ice accretion on a swept wing at glaze ice conditions. (a) Attachment line zone, glaze ice feathers zone, and critical distance (view from direction normal to leading edge). (b) Attachment line zone, glaze ice feathers zone, and critical distance (overall view)

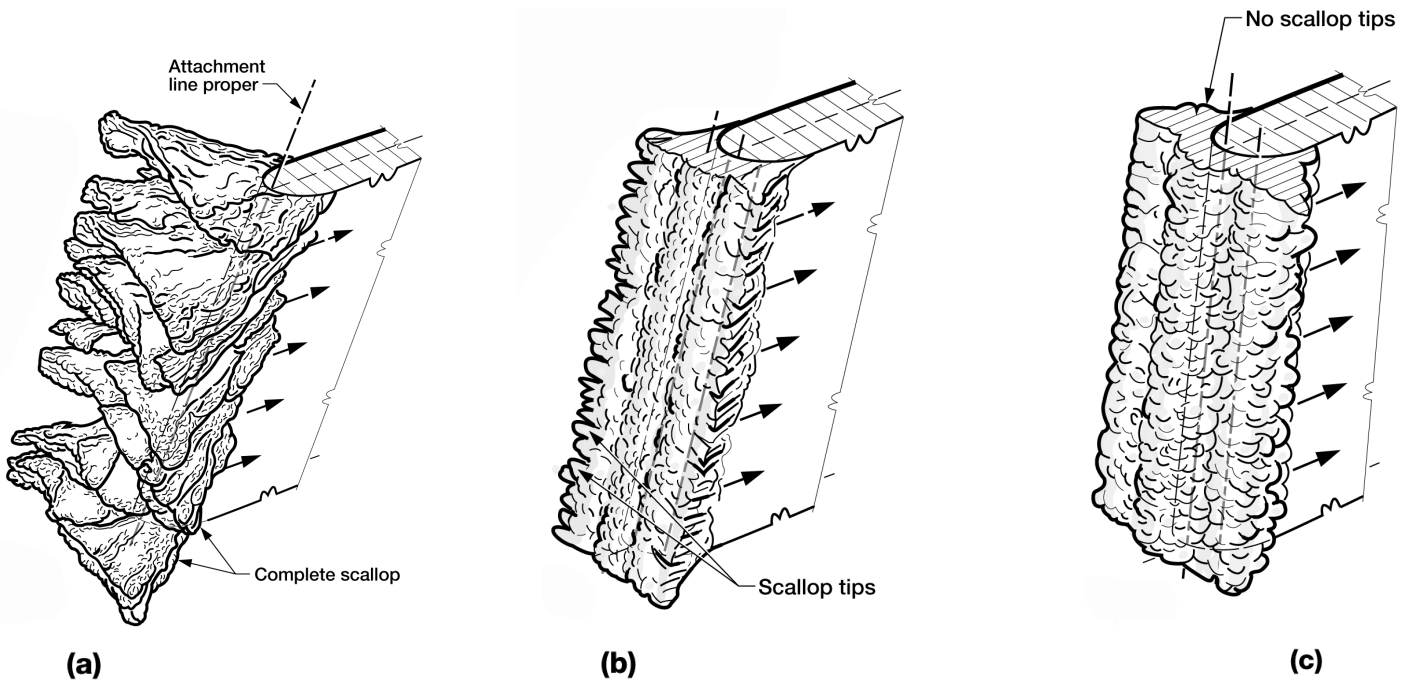


Figure 2. Ice accretion on a swept wing at glaze ice conditions. (a) Complete scallop case, critical distance = 0. (b) Incomplete scallop case, critical distance > 0, scallop tips are formed at a given distance (the critical distance) from the attachment line proper. (c) No-scallop case, critical distance > 0, scallop tips are not formed.



Figure 3. NASA Glenn Research Center Icing Research Aircraft (DHC-6 Twin Otter Aircraft)

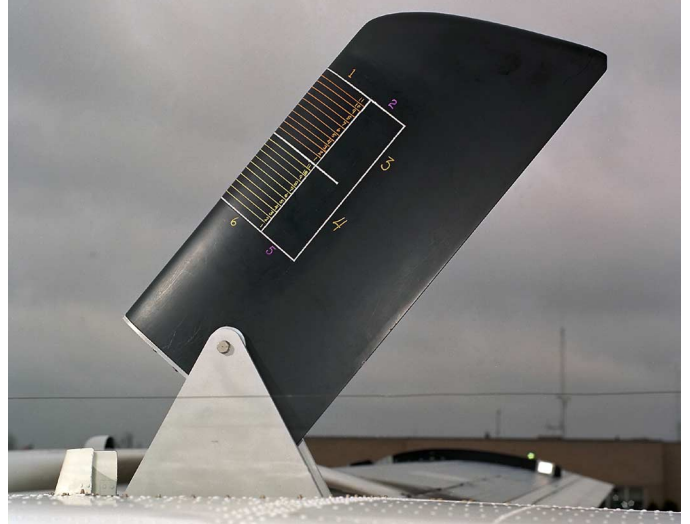


Figure 4. NACA 0012 Swept Wing Tip airfoil

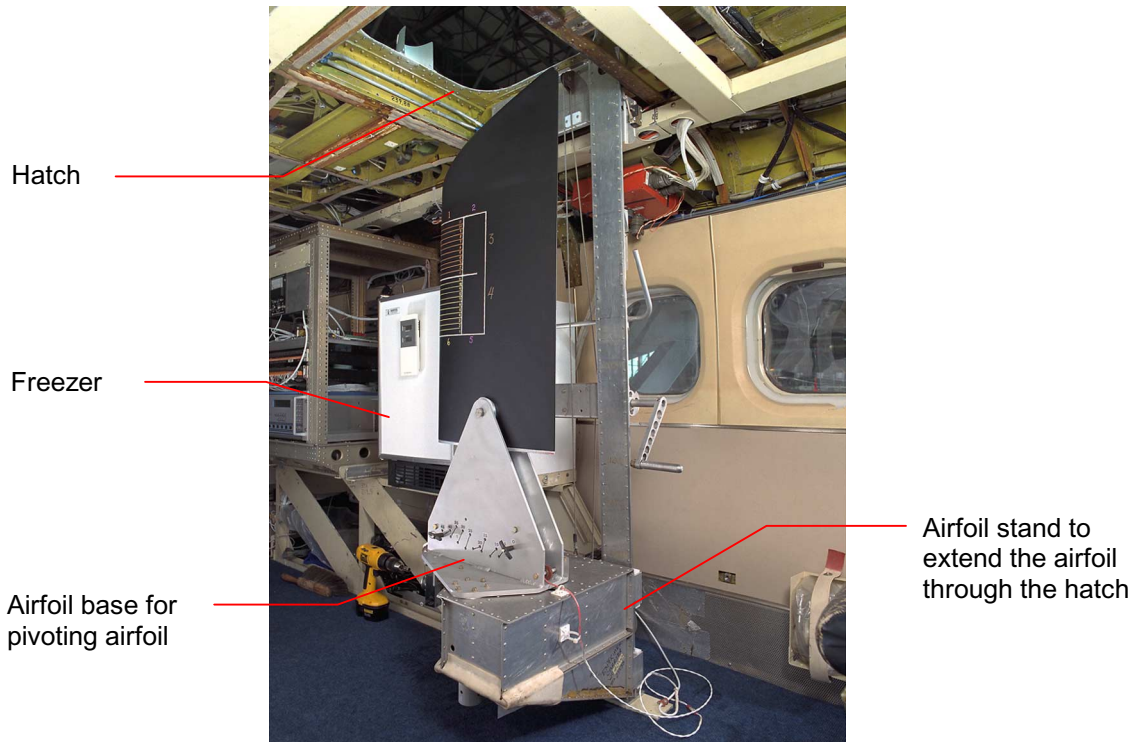


Figure 5. View of experimental hardware inside the cabin of the aircraft

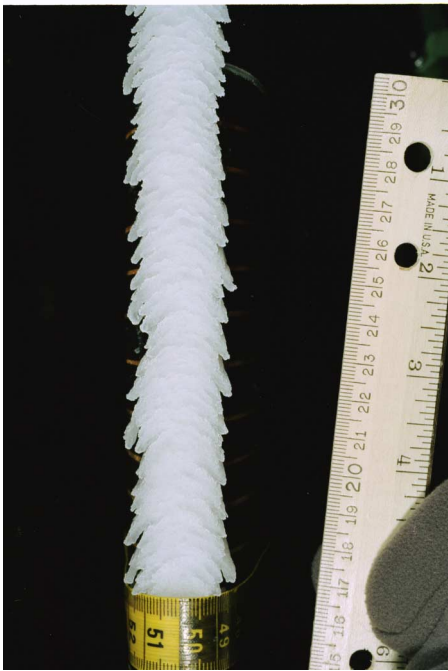


Figure 6. Front view of ice accretion showing complete scallops. Twin Otter aircraft run number 012401.01, average conditions: $\Lambda = 45^\circ$, $V = 142$ mph, $T_{\text{total}} = 24.8^\circ\text{F}$, $T_{\text{static}} = 21.0^\circ\text{F}$, $\text{LWC} = 0.48\text{g/m}^3$, $\text{MVD} = 12.3\mu\text{m}$, $\tau = 10\text{min}$. Direction of flow is from bottom to top; scale of ruler is in centimeters, smallest division 1 mm.



Figure 7. Front view of ice accretion showing complete scallops. Twin Otter aircraft run number 013101.01, average conditions: $\Lambda = 45^\circ$, $V = 142$ mph, $T_{\text{total}} = 26.6^\circ\text{F}$, $T_{\text{static}} = 22.8^\circ\text{F}$, $\text{LWC} = 0.37\text{g/m}^3$, $\text{MVD} = 12.2\mu\text{m}$, $\tau = 6\text{min}$. Direction of flow is from bottom to top; scale of ruler is in centimeters, smallest division 1 mm.

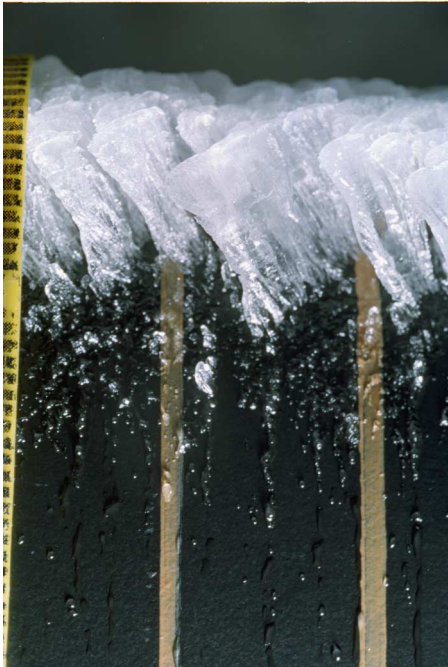


Figure 8. Side view of ice accretion showing feather formation of scallop tips. Twin Otter aircraft run number 013101.01, average conditions: $\Lambda = 45^\circ$, $V = 142$ mph, $T_{\text{total}} = 26.6^\circ\text{F}$, $T_{\text{static}} = 22.8^\circ\text{F}$, $\text{LWC} = 0.37\text{g/m}^3$, $\text{MVD} = 12.2\mu\text{m}$, $\tau = 6\text{min}$. Direction of flow is from left to right; scale of ruler is in centimeters, smallest division 1 mm.



Figure 9. Front view of ice accretion obtained in the Icing Research Tunnel showing complete scallops. $\Lambda = 45^\circ$, $V = 150$ mph, $T_{\text{total}} = 25^\circ\text{F}$, $\text{LWC} = 0.5\text{g/m}^3$, $\text{MVD} = 20\mu\text{m}$, $\tau = 5\text{min}$. Direction of flow is from bottom to top; scale of ruler is in centimeters, smallest division 1 mm.



Figure 10. Close-up of in-flight ice accretion shown in Figures 7. Run number 013101.01, average conditions: $\Lambda = 45^\circ$, $V = 142$ mph, $T_{\text{total}} = 26.6^\circ\text{F}$, $T_{\text{static}} = 22.8^\circ\text{F}$, $\text{LWC} = 0.37\text{g/m}^3$, $\text{MVD} = 12.2\mu\text{m}$, $\tau = 6\text{min}$. Direction of flow is from bottom to top; scale of ruler is in centimeters, smallest division 1 mm.



Figure 11. Close-up of Icing Research Tunnel ice accretion shown in Figure 9. $\Lambda = 45^\circ$, $V = 150$ mph, $T = 25^\circ\text{F}$, $\text{LWC} = 0.5\text{g/m}^3$, $\text{MVD} = 20\mu\text{m}$, $\tau = 5\text{min}$. Direction of flow is from bottom to top; scale of ruler is in centimeters, smallest division 1 mm.



Figure 12. Front view of ice accretion showing complete scallops. Twin Otter aircraft run number 013101.02, average conditions: $\Lambda = 30^\circ$, $V = 144$ mph, $T_{\text{total}} = 25.3^\circ\text{F}$, $T_{\text{static}} = 21.2^\circ\text{F}$, $\text{LWC} = 0.45\text{g/m}^3$, $\text{MVD} = 13.3\mu\text{m}$, $\tau = 8\text{min}$. Direction of flow is from bottom to top; scale of ruler is in centimeters, smallest division 1 mm.



Figure 13. Front view of ice accretion obtained in the Icing Research Tunnel, showing complete scallops. $\Lambda = 30^\circ$, $V = 150$ mph, $T = 25^\circ\text{F}$, $\text{LWC} = 0.5\text{g/m}^3$, $\text{MVD} = 20\mu\text{m}$, $\tau = 10\text{min}$. Direction of flow is from bottom to top; scale of ruler is in inches, smallest division 1/16 of an inch.



Figure 14. Front view of no-scallop ice accretion showing attachment line zone and glaze ice feathers zone. Twin Otter aircraft run number 013101.03, average conditions: $\Lambda = 15^\circ$, $V = 143$ mph, $T_{\text{total}} = 25.9^\circ\text{F}$, $T_{\text{static}} = 21.9^\circ\text{F}$, $\text{LWC} = 0.39\text{g/m}^3$, $\text{MVD} = 12.3\mu\text{m}$, $\tau = 8\text{min}$. Direction of flow is from bottom to top; scale of ruler is in centimeters, smallest division 1 mm.

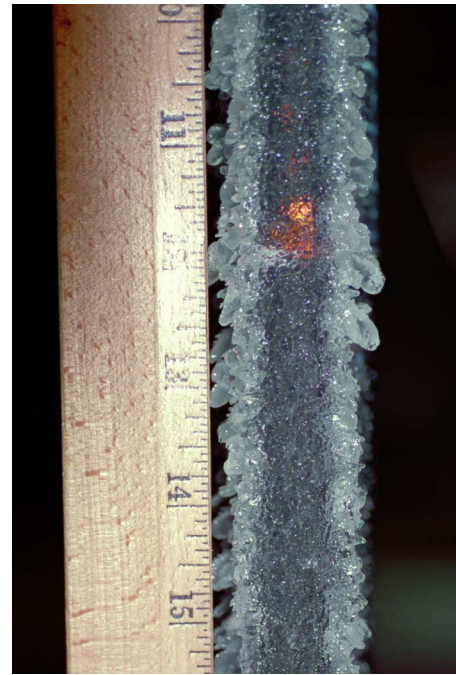


Figure 15. Front view of no-scallop ice accretion obtained in the Icing Research Tunnel. $\Lambda = 15^\circ$, $V = 150$ mph, $T = 25^\circ\text{F}$, $\text{LWC} = 0.5\text{g/m}^3$, $\text{MVD} = 20\mu\text{m}$, $\tau = 10\text{min}$. Direction of flow is from bottom to top; scale of ruler is in inches, smallest division 1/16 of an inch.



Figure 16. Front view of no-scallop ice accretion showing attachment line zone and glaze ice feathers zone. Twin Otter aircraft run number 013101.04, average conditions: $\Lambda = 0^\circ$, $V = 142$ mph, $T_{\text{total}} = 26.4^\circ\text{F}$, $T_{\text{static}} = 21.7^\circ\text{F}$, $\text{LWC} = 0.41\text{g/m}^3$, $\text{MVD} = 13.1\mu\text{m}$, $\tau = 7\text{min}$. Direction of flow is from bottom to top; scale of ruler is in centimeters, smallest division 1 mm.

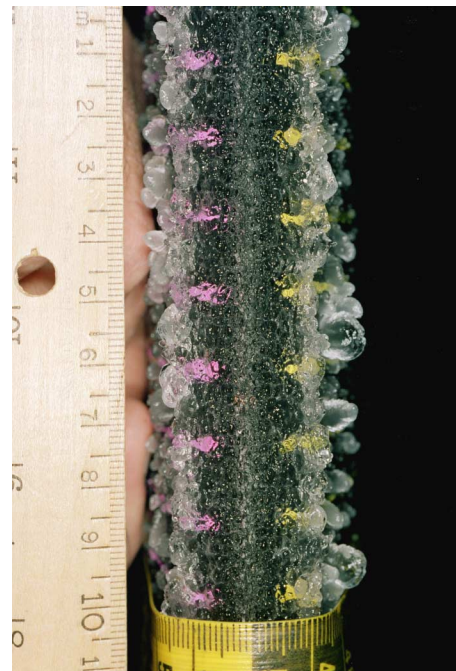


Figure 17. Front view of no-scallop ice accretion obtained in the Icing Research Tunnel. $\Lambda = 0^\circ$, $V = 150$ mph, $T = 25^\circ\text{F}$, $\text{LWC} = 0.5\text{g/m}^3$, $\text{MVD} = 20\mu\text{m}$, $\tau = 5\text{min}$. Direction of flow is from bottom to top; scale of ruler is in centimeters, smallest division 1 mm.



Figure 18. Front view of complete scallops on the end cap of the airfoil for the ice accretion shown in Figure 14. Twin Otter aircraft run number 013101.03, average conditions: $\Lambda = 15^\circ$, $V = 143$ mph, $T_{total} = 25.9^\circ\text{F}$, $T_{static} = 21.9^\circ\text{F}$, $LWC = 0.39\text{g/m}^3$, $MVD = 12.3\mu\text{m}$, $\tau = 8\text{min}$. Direction of flow is from bottom to top; scale of ruler is in centimeters, smallest division 1 mm.



Figure 19. Side view of Figure 18, complete scallops on the end cap of the airfoil showing feather formation. Twin Otter aircraft run number 013101.03, average conditions: $\Lambda = 15^\circ$, $V = 143$ mph, $T_{total} = 25.9^\circ\text{F}$, $T_{static} = 21.9^\circ\text{F}$, $LWC = 0.39\text{g/m}^3$, $MVD = 12.3\mu\text{m}$, $\tau = 8\text{min}$. Direction of flow is from left to right; scale of ruler is in centimeters, smallest division 1 mm.



Figure 20. Front view of ice accretion showing complete scallops. Twin Otter aircraft run number 011901.03, average conditions: $\Lambda = 45^\circ$, $V = 143$ mph, $T_{total} = 25.0^\circ\text{F}$, $T_{static} = 21.2^\circ\text{F}$, $LWC = 0.33\text{g/m}^3$, $MVD = 14.0\mu\text{m}$, $\tau = 14\text{min}$. Direction of flow is from bottom to top; scale of ruler is in centimeters, smallest division 1 mm.



Figure 21. Front view of ice accretion showing complete scallops. Twin Otter aircraft run number 012601.02, average conditions: $\Lambda = 30^\circ$, $V = 139$ mph, $T_{total} = 26.2^\circ\text{F}$, $T_{static} = 22.3^\circ\text{F}$, $LWC = 0.32\text{g/m}^3$, $MVD = 13.5\mu\text{m}$, $\tau = 12\text{min}$. Direction of flow is from bottom to top; scale of ruler is in centimeters, smallest division 1 mm.



Figure 22. Front view of incomplete scallops showing attachment line zone and glaze ice feathers zone. Twin Otter aircraft run number 013101.05, average conditions: $\Lambda = 25^\circ$, $V = 143$ mph, $T_{\text{total}} = 26.1^\circ\text{F}$, $T_{\text{static}} = 22.1^\circ\text{F}$, $\text{LWC} = 0.32\text{g/m}^3$, $\text{MVD} = 12.2\mu\text{m}$, $\tau = 7\text{min}$. Direction of flow is from bottom to top; scale of ruler is in centimeters, smallest division 1 mm.

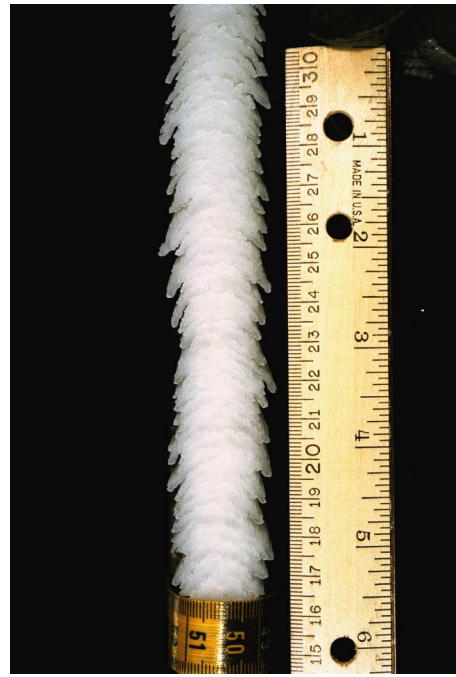


Figure 23. Front view of ice accretion showing complete scallops. Twin Otter aircraft run number 012401.07, average conditions: $\Lambda = 45^\circ$, $V = 144$ mph, $T_{\text{total}} = 19.3^\circ\text{F}$, $T_{\text{static}} = 15.4^\circ\text{F}$, $\text{LWC} = 0.40\text{g/m}^3$, $\text{MVD} = 11.8\mu\text{m}$, $\tau = 13\text{min}$. Direction of flow is from bottom to top; scale of ruler is in centimeters, smallest division 1 mm.

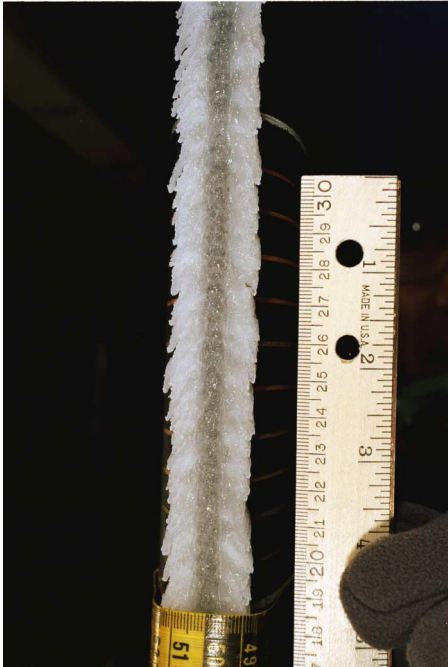


Figure 24. Front view of incomplete scallops showing attachment line zone and glaze ice feathers zone. Twin Otter aircraft run number 012401.02, average conditions: $\Lambda = 30^\circ$, $V = 144$ mph, $T_{\text{total}} = 22.1^\circ\text{F}$, $T_{\text{static}} = 18.1^\circ\text{F}$, $\text{LWC} = 0.54\text{g/m}^3$, $\text{MVD} = 12.8\mu\text{m}$, $\tau = 13\text{min}$. Direction of flow is from bottom to top; scale of ruler is in centimeters, smallest division 1 mm.



Figure 25. Close-up of ice accretion from Figure 24, showing attachment line covered with ice. Twin Otter aircraft run number 012401.02, average conditions: $\Lambda = 30^\circ$, $V = 144$ mph, $T_{\text{total}} = 22.1^\circ\text{F}$, $T_{\text{static}} = 18.1^\circ\text{F}$, $\text{LWC} = 0.54\text{g/m}^3$, $\text{MVD} = 12.8\mu\text{m}$, $\tau = 13\text{min}$. Direction of flow is from bottom to top; scale of ruler is in centimeters, smallest division 1 mm.



Figure 26. Side view of ice accretion from Figure 24, showing tightly packed feathers. Twin Otter aircraft run number 012401.02, average conditions: $\Lambda = 30^\circ$, $V = 144$ mph, $T_{\text{total}} = 22.1^\circ\text{F}$, $T_{\text{static}} = 18.1^\circ\text{F}$, $\text{LWC} = 0.54\text{g/m}^3$, $\text{MVD} = 12.8\mu\text{m}$, $\tau = 13\text{min}$. Direction of flow is from left to right; scale of ruler is in centimeters. smallest division 1 mm.

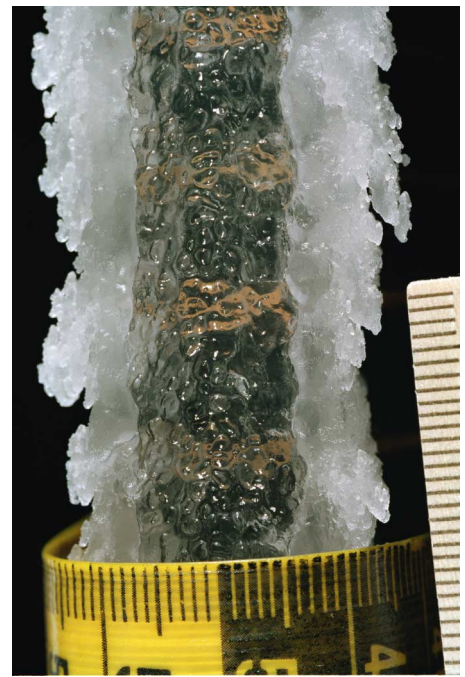


Figure 27. Front view of no-scallop ice accretion showing attachment line zone and glaze ice feathers zone. Twin Otter aircraft run number 012401.03, average conditions: $\Lambda = 15^\circ$, $V = 143$ mph, $T_{\text{total}} = 20.5^\circ\text{F}$, $T_{\text{static}} = 16.7^\circ\text{F}$, $\text{LWC} = 0.51\text{g/m}^3$, $\text{MVD} = 12.6\mu\text{m}$, $\tau = 10\text{min}$. Direction of flow is from bottom to top; scale of ruler is in centimeters, smallest division 1 mm.



Figure 28. Front view of no-scallop ice accretion showing attachment line zone and glaze ice feathers zone. Twin Otter aircraft run number 012401.04, average conditions: $\Lambda = 0^\circ$, $V = 142$ mph, $T_{\text{total}} = 21.2^\circ\text{F}$, $T_{\text{static}} = 17.4^\circ\text{F}$, $\text{LWC} = 0.46\text{g/m}^3$, $\text{MVD} = 12.1\mu\text{m}$, $\tau = 9\text{min}$. Direction of flow is from bottom to top; scale of ruler is in centimeters, smallest division 1 mm.

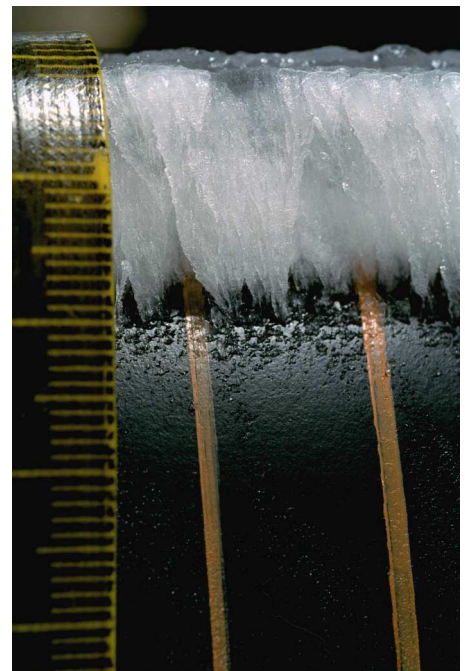


Figure 29. Side view of ice accretion from showing tightly packed feathers. Twin Otter aircraft run number 012401.03, average conditions: $\Lambda = 15^\circ$, $V = 143$ mph, $T_{\text{total}} = 20.5^\circ\text{F}$, $T_{\text{static}} = 16.7^\circ\text{F}$, $\text{LWC} = 0.51\text{g/m}^3$, $\text{MVD} = 12.6\mu\text{m}$, $\tau = 10\text{min}$. Direction of flow is from left to right; scale of ruler is in centimeters, smallest division 1 mm.



Figure 30. Front view of ice accretion showing complete scallops. Twin Otter aircraft run number 012601.01, average conditions: $\Lambda = 45^\circ$, $V = 159$ mph, $T_{\text{total}} = 30.6^\circ\text{F}$, $T_{\text{static}} = 25.5^\circ\text{F}$, $\text{LWC} = 0.36\text{g/m}^3$, $\text{MVD} = 14.4\mu\text{m}$, $\tau = 9\text{min}$. Direction of flow is from bottom to top; scale of ruler is in centimeters, smallest division 1 mm.



Figure 31. Front view of ice accretion showing complete scallops. Twin Otter aircraft run number 013001.01, average conditions: $\Lambda = 45^\circ$, $V = 148$ mph, $T_{\text{total}} = 29.3^\circ\text{F}$, $T_{\text{static}} = 24.1^\circ\text{F}$, $\text{LWC} = 0.13\text{g/m}^3$, $\text{MVD} = 14.9\mu\text{m}$, $\tau = 41\text{min}$. Direction of flow is from bottom to top; scale of ruler is in centimeters, smallest division 1 mm.



Figure 32. Front view of no-scallop ice accretion showing attachment line zone and glaze ice feathers zone. Twin Otter aircraft run number 012601.03, average conditions: $\Lambda = 0^\circ$, $V = 138$ mph, $T_{\text{total}} = 30.2^\circ\text{F}$, $T_{\text{static}} = 26.4^\circ\text{F}$, $\text{LWC} = 0.31\text{g/m}^3$, $\text{MVD} = 12.0\mu\text{m}$, $\tau = 12\text{min}$. Direction of flow is from bottom to top; scale of ruler is in centimeters, smallest division 1 mm.



Figure 33. Front view of no-scallop ice accretion showing attachment line zone and glaze ice feathers zone. Twin Otter aircraft run number 011801.01, average conditions: $\Lambda = 0^\circ$, $V = 151$ mph, $T_{\text{total}} = 16.9^\circ\text{F}$, $T_{\text{static}} = 11.1^\circ\text{F}$, $\text{LWC} = 0.10\text{g/m}^3$, $\text{MVD} = 11.0\mu\text{m}$, $\tau = 15\text{min}$. Direction of flow is from bottom to top; scale of ruler is in centimeters, smallest division 1 mm.



Figure 34. Front view of no-scallop ice accretion showing attachment line zone and glaze ice feathers zone. Twin Otter aircraft run number 011901.05, average conditions: $\Lambda = 15^\circ$, $V = 137$ mph, $T_{total} = 19.4^\circ\text{F}$, $T_{static} = 14.9^\circ\text{F}$, $LWC = 0.16\text{g/m}^3$, $MVD = 14.0\mu\text{m}$, $\tau = 18\text{min}$. Direction of flow is from bottom to top; scale of ruler is in centimeters, smallest division 1 mm.

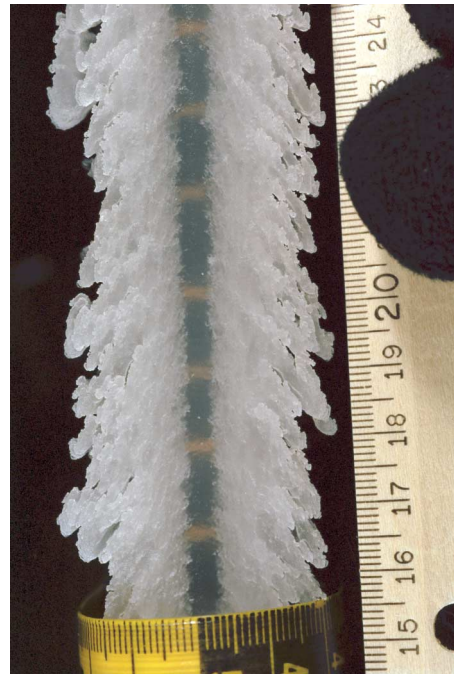


Figure 35. Front view of incomplete scallops showing attachment line zone and glaze ice feathers zone. Twin Otter aircraft run number 011901.04, average conditions: $\Lambda = 30^\circ$, $V = 142$ mph, $T_{total} = 19.6^\circ\text{F}$, $T_{static} = 15.6^\circ\text{F}$, $LWC = 0.20\text{g/m}^3$, $MVD = 15.0\mu\text{m}$, $\tau = 19\text{min}$. Direction of flow is from bottom to top; scale of ruler is in centimeters, smallest division 1 mm.



Figure 36. Side view of no-scallop ice accretion showing tightly packed feathers. Twin Otter aircraft run number 012401.05, average conditions: $\Lambda = 0^\circ$, $V = 146$ mph, $T_{total} = 20.0^\circ\text{F}$, $T_{static} = 16.0^\circ\text{F}$, $LWC = 0.28\text{g/m}^3$, $MVD = 10.2\mu\text{m}$, $\tau = 16\text{min}$. Direction of flow is from bottom to top; scale of ruler is in centimeters, smallest division 1 mm.



Figure 37. Front view of incomplete scallops showing attachment line zone and glaze ice feathers zone. Twin Otter aircraft run number 011901.02, average conditions: $\Lambda = 45^\circ$, $V = 132$ mph, $T_{total} = 18.3^\circ\text{F}$, $T_{static} = 13.6^\circ\text{F}$, $LWC = 0.07\text{g/m}^3$, $MVD = 17.0\mu\text{m}$, $\tau = 22\text{min}$. Direction of flow is from bottom to top; scale of ruler is in centimeters, smallest division 1 mm.



Figure 38. Side view of ice accretion showing tightly packed feathers. Twin Otter aircraft run number 012201.01, average conditions: $\Lambda = 45^\circ$, $V = 159$ mph, $T_{\text{total}} = 18.9^\circ\text{F}$, $T_{\text{static}} = 14.2^\circ\text{F}$, $\text{LWC} = 0.14\text{g/m}^3$, $\text{MVD} = 9.0\mu\text{m}$, $\tau = 25\text{min}$. Direction of flow is from bottom to top; scale of ruler is in centimeters, smallest division 1 mm.

REPORT DOCUMENTATION PAGEForm Approved
OMB No. 0704-0188

Public reporting burden for this collection of information is estimated to average 1 hour per response, including the time for reviewing instructions, searching existing data sources, gathering and maintaining the data needed, and completing and reviewing the collection of information. Send comments regarding this burden estimate or any other aspect of this collection of information, including suggestions for reducing this burden, to Washington Headquarters Services, Directorate for Information Operations and Reports, 1215 Jefferson Davis Highway, Suite 1204, Arlington, VA 22202-4302, and to the Office of Management and Budget, Paperwork Reduction Project (0704-0188), Washington, DC 20503.

1. AGENCY USE ONLY (Leave blank)		2. REPORT DATE January 2002	3. REPORT TYPE AND DATES COVERED Technical Memorandum	
4. TITLE AND SUBTITLE Ice Accretion Formations on a NACA 0012 Swept Wing Tip in Natural Icing Conditions			5. FUNDING NUMBERS WU-711-20-23-00	
6. AUTHOR(S) Mario Vargas, Julius A. Giriunas, and Thomas P. Ratvasky				
7. PERFORMING ORGANIZATION NAME(S) AND ADDRESS(ES) National Aeronautics and Space Administration John H. Glenn Research Center at Lewis Field Cleveland, Ohio 44135-3191			8. PERFORMING ORGANIZATION REPORT NUMBER E-13175	
9. SPONSORING/MONITORING AGENCY NAME(S) AND ADDRESS(ES) National Aeronautics and Space Administration Washington, DC 20546-0001			10. SPONSORING/MONITORING AGENCY REPORT NUMBER NASA TM-2002-211357 AIAA-2002-0244	
11. SUPPLEMENTARY NOTES Prepared for the 40th Aerospace Sciences Meeting and Exhibit sponsored by the American Institute of Aeronautics and Astronautics, Reno, Nevada, January 14-17, 2002. Responsible person, Mario Vargas, organization code 5840, 216-433-3943.				
12a. DISTRIBUTION/AVAILABILITY STATEMENT Unclassified - Unlimited Subject Categories: 01 and 34 Available electronically at http://gltrs.grc.nasa.gov/GLTRS This publication is available from the NASA Center for AeroSpace Information, 301-621-0390.			12b. DISTRIBUTION CODE	
13. ABSTRACT (Maximum 200 words) An experiment was conducted in the DeHavilland DHC-6 Twin Otter Icing Research Aircraft at NASA Glenn Research Center to study the formation of ice accretions on swept wings in natural icing conditions. The experiment was designed to obtain ice accretion data to help determine if the mechanisms of ice accretion formation observed in the Icing Research Tunnel are present in natural icing conditions. The experiment in the Twin Otter was conducted using a NACA 0012 swept wing tip. The model enabled data acquisition at 0°, 15°, 25°, 30°, and 45° sweep angles. Casting data, ice shape tracings, and close-up photographic data were obtained. The results showed that the mechanisms of ice accretion formation observed in-flight agree well with the ones observed in the Icing Research Tunnel. Observations on the end cap of the airfoil showed the same strong effect of the local sweep angle on the formation of scallops as observed in the tunnel.				
14. SUBJECT TERMS Ice formation; Swept wings			15. NUMBER OF PAGES 29	
			16. PRICE CODE	
17. SECURITY CLASSIFICATION OF REPORT Unclassified	18. SECURITY CLASSIFICATION OF THIS PAGE Unclassified	19. SECURITY CLASSIFICATION OF ABSTRACT Unclassified	20. LIMITATION OF ABSTRACT	